Advances in modelling of laser induced cavitation bubble dynamics and cavitation shock waves with the Finite Volume Method

Max Koch[1], Christiane Lechner[2], Fabian Reuter[1], Robert Mettin[1], Werner Lauterborn[1]

[1] *Christian Doppler Laboratory for Cavitation and Micro-Erosion, Drittes Physikalisches Institut, Georg-August-Universität Göttingen, Friedrich-Hund-Platz 1, 37077 Göttingen, Germany, Email: max.koch@stud.uni-goettingen.de, RMettin@gwdg.de*

[2] *Institute of Fluid Mechanics and Heat Transfer, TU Wien, Getreidemarkt 9, 1060 Vienna, Austria*

Introduction

First results of the dynmics of a cavitation bubble in front of a rigid wall are presented, obtained by advanced numerical calculations with a Finite Volume solver. The solver is based on the algorithm *compressibleInterFoam* of the open source package OpenFOAM [1, 2]. The modifications that were implemented for the application to cavitation bubbles, as well as solver validations, are described in detail in [3]. The solver was found to be robust against the demands of cavitation bubble dynamics, also upon strong collapse, which are mainly: i) the span of the bubble pressure over 10 orders of magnitude, ii) the span of the bubble radius over 2 orders of magnitude, iii) the nonlinear compressibility effects such as shock wave emission, iv) and topology changes of the bubble during an aspherical collapse. In this paper, the bubble consists of non-condensible gas without vapour and it is surrounded by water. Condensation and evaporation of the liquid phase, as well as diffusion of the gas, are neglected.

Brief description of the solver

With the Finite Volume method, the computational domain is discretized into finite volume cells. In this way, gradient (∇) and divergence ($\nabla\cdot$) terms can be rewritten by means of sums over the surfaces of the cells. The governing physical equations that are solved are the Navier-Stokes equation (1), supplemented by the continuity equation (2) as well as the continuity equation for one phase α_i (3) and the two equations of state for the gas and liquid (4,5), respectively.

$$\frac{\partial(\rho\,\mathbf{U})}{\partial t} + \nabla\cdot(\rho\,\mathbf{U}\otimes\mathbf{U}) = -\nabla p + \nabla\cdot\mathbb{T} + \text{surface tension term}, \tag{1}$$

$$\frac{\partial\rho}{\partial t} + \nabla\cdot(\rho\,\mathbf{U}) = 0\,, \tag{2}$$

$$\frac{\partial(\alpha_i\rho_i)}{\partial t} + \nabla\cdot(\alpha_i\rho_i\mathbf{U}) = 0\,, \qquad i = l, g\,, \tag{3}$$

$$p\left(\frac{1}{\rho} - \frac{\beta}{\rho_\mathrm{n}}\right)^{\gamma} = \text{const}, \tag{4}$$

$$p(\rho) = (p_\infty + B)\left(\frac{\rho}{\rho_\infty}\right)^{n_T} - B\,. \tag{5}$$

$\mathbb{T}$ is the viscous stress tensor of a Newtonian fluid,

$$\mathbb{T} := \mu\left(\nabla\mathbf{U} + (\nabla\mathbf{U})^T - \frac{2}{3}(\nabla\cdot\mathbf{U})\,\mathbb{I}\right), \tag{6}$$

with $\mathbb{I}$ the unit tensor. The surface tension coefficient of the liquid/gas interface is taken to be constant. The exact formulation for the surface tension term is omitted here for the sake of simplicity. See [4] and [3] for detailed explanation. The phases are distinguished via the field $\alpha \in [0, 1]$, where $\alpha = 0$ for the gas and $\alpha = 1$ for the liquid, and therefore $\alpha_l = 1 - \alpha_g$. γ denotes the ratio of specific heats. We use $\gamma = 1.4$ for air or any two-atomic molecule gas under adiabatic compression. β is the co-volume de-dimensionalized with the molar volume at equilibrium (see necessity for β in [5]). For the liquid, the Tait-equation of state for water (5) is used [6] with p_∞ the atmospheric pressure and ρ_∞ the equilibrium density.

A very rough sketch [3] of the sequence of the solver is given below (upper index k denoting the time step):

1. Solve the propagation equation for α_l
2. Compute surface tension force
3. Solve (1) for a predictor $\widetilde{\mathbf{U}}^k$ using p^k and the new surface force term.
4. Solve (3) rewritten for the pressure
5. Update $\mathbf{U}^{k+1}$
6. Compute ρ_i^{k+1}
7. Correct the mass of the bubble
8. Update $\rho^{k+1} = \alpha_g^{k+1}\rho_g^{k+1} + \alpha_l^{k+1}\rho_l^{k+1}$

Results

Figures 1 – 5 show the results of the calculations over the life time of the bubble at different stages, where different effects occur. The calculation was done in axial symmetry and the visualization in the figures is done in a split manner: For each frame or time step the left side shows the velocity field around the bubble with arrows for the direction and coloured background for the logarithmic magnitude. The velocity field of the interior of the bubble itself is masked (light blue), since it varies a lot without any effect on the general dynamics. Furthermore, the masking depicts the bubble shape more clearly. The right side of each frame shows the pressure field in logarithmic scale, with different intervals as indicated.

The bubble distance to the wall is 641.55 µm and

the maximum radius is 550 µm, giving a dimensionless standoff-parameter $\gamma_s \approx 1.17$. The starting radius is 24 µm, the bubble radius at equilibrium is varied over time: it starts at 200 µm and decays to 80 µm within 30 µs, where it stays. The equilibrium radius is a measure for the amount of gas inside the bubble. This procedure has been chosen to mimic a laser induced breakdown scenario.

The dynamics of a laser induced cavitation bubble in front of a rigid wall can be simulated in detail with the solver introduced in [3]. The very first expansion phase of the bubble (1.3 µs) with shock wave emission and the subsequent reflections of the wave at the solid boundary and the bubble are shown in Fig. 1. The further expansion up to a maximum radius of 550 µm and the subsequent collapse from an intermediately reached oblong shape with liquid jet formation is given in Fig. 2. The succession of phenomena after liquid jet impact on the opposite bubble wall is quite complex and difficult to simulate as the violence of the events provokes instabilities. This may lead to the formation of some tiny (torus) bubbles near the location of jet impact. They soon disappear except for one near the boundary. A robust phenomenon is "splashing" [7, 8], i.e. a ring water wave emanating from the point of jet impact. The jet displaces water that piles up like a water wave when a stone is thrown into a pond, just that it is kept inside the bubble with its curved surface. This splash or water wave in the bubble is seen in Fig. 3 at 117.1996 µs. As the torus bubble collapses further after jet impact, the splash peak height may touch the inner torus side thus splitting the torus into two tori. The two tori and the one from immediate jet impact collapse further with the emission of a torus shock wave each (Fig. 3, 117.5796 µs – 118.0354 µs). A complicated shock and expansion wave as well as flow field is set up. Upon first rebound the tori disappear or merge, expand to some maximum size and collapse again, this time on the surface (Fig. 4). After second collapse the bubble disintegrates (Fig. 4 and 5) and a flow upwards with vortices going upwards away from the surface develops. This scenario is also observed experimentally: Fig. 6 shows a slightly smaller laser induced bubble ($R_{\max} = 450\,\mu\text{m}$) with comparable standoff-parameter $\gamma_s \simeq 1.2$ which was observed with a high speed camera. It especially shows the same phenomenon of some remnant bubbles moving away from the wall at the end of the whole process.

Conclusion and Outlook

Expansion and collapse shock waves are captured and the torus formation during jet impact with subsequent splitting into several tori, due to "splashing" can be seen. The flows and flow vortices that evolve after first and second collapse are considered to be physically relevant, e.g. for surface cleaning [9] or erosion [10]. We conclude that with this solver a wide range of single cavitation bubble dynamics can be captured very well and further tests against experimental results are in progress.

Acknowledgements

The financial support by the Austrian Federal Ministry of Economy, Family and Youth and the National Foundation for Research, Technology and Development is gratefully acknowledged.

References

[1] S.T. Miller, H. Jasak, D.A. Boger, E.G. Paterson and A. Nedungadi. 'A pressure-based, compressible, two-phase flow finite volume method for underwater explosions'. In: *Computers & Fluids* 87 (2013), pp. 132–143.

[2] OpenFOAM-extend project community. *OpenFOAM-extend project.* Download at http://sourceforge.net/projects/openfoam-extend/files/foam-extend-3.0/. July 2014.

[3] M. Koch, C. Lechner, F. Reuter, K. Köhler, R. Mettin and W. Lauterborn. 'Numerical modelling of laser generated cavitation bubbles with the finite volume and volume of fluid method, using OpenFOAM'. In: *Computers & Fluids* 126 (2016), pp. 71 –90.

[4] G. Tryggvason, B. Bunner, A. Esmaeeli, D. Juric, N. Al-Rawahi, W. Tauber, J. Han, S. Nas and Y.-J. Jan. 'A Front-Tracking Method for the Computations of Multiphase Flow'. In: *Journal of Computational Physics* 169 (2001), pp. 708–759.

[5] Ritva Löfstedt, Bradley P. Barber and Seth J. Putterman. 'Toward a hydrodynamic theory of sonoluminescence'. In: *Physics of Fluids* A 5.11 (1993), pp. 2911–2928.

[6] Yuan-Hui Li. 'Equations of State of Water and Sea Water'. In: *Journal of Geophysical Research* 72.10 (1967), pp. 2665–2678.

[7] R. P. Tong, W. P. Schiffers, S. J. Shaw, J. R. Blake and D. C. Emmony. 'The role of 'splashing' in the collapse of a laser-generated cavity near a rigid boundary'. In: *Journal of Fluid Mechanics* 380 (Feb. 1999), pp. 339–361.

[8] A. M. Zhang, S. Li and J. Cui. 'Study on splitting of a toroidal bubble near a rigid boundary'. In: *Physics of Fluids* 27.6, 062102 (2015).

[9] Fabian Reuter and Robert Mettin. 'Mechanisms of single bubble cleaning'. In: *Ultrasonics Sonochemistry* 29 (2016), pp. 550 –562.

[10] A. Philipp and W. Lauterborn. 'Cavitation erosion by single laser-produced bubbles'. In: *Journal of Fluid Mechanics* 361 (1998), pp. 75–116.

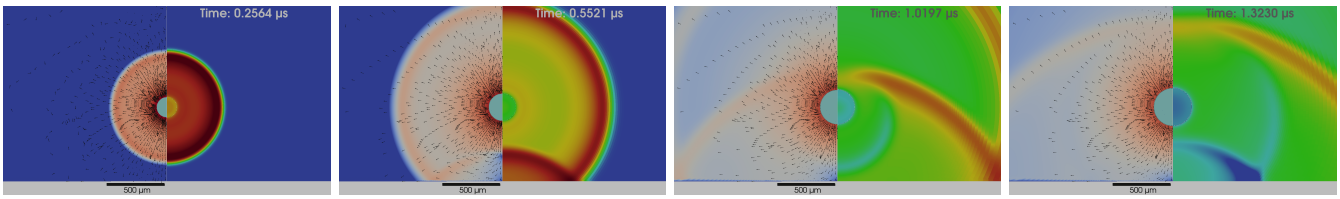

$t = 0.2564\,\mu s$ 0.5521 µs 1.0197 µs 1.3230 µs

Figure 1: First 1.323 µs of the bubble expansion phase with shock wave emission, sound hard and sound soft reflection at the solid boundary below and at the bubble, respectively; the black bar on the bottom of the left frame denotes 500 µm length; scales are the same as in Fig. 3

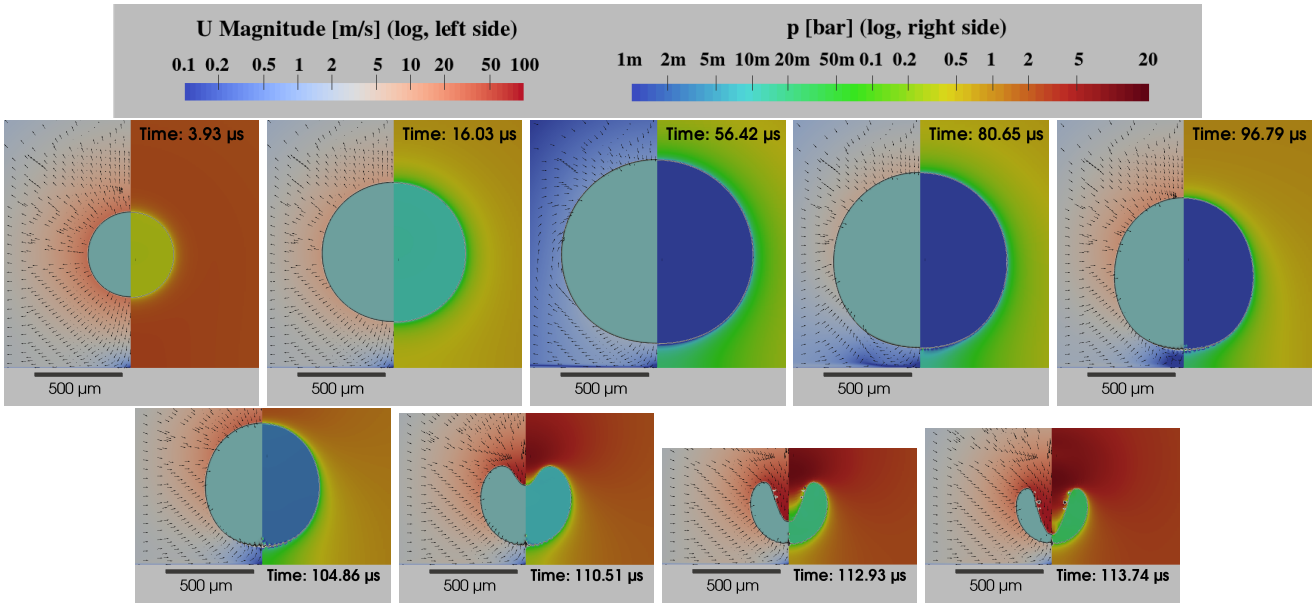

Figure 2: First expansion and first collapse phase with jet formation

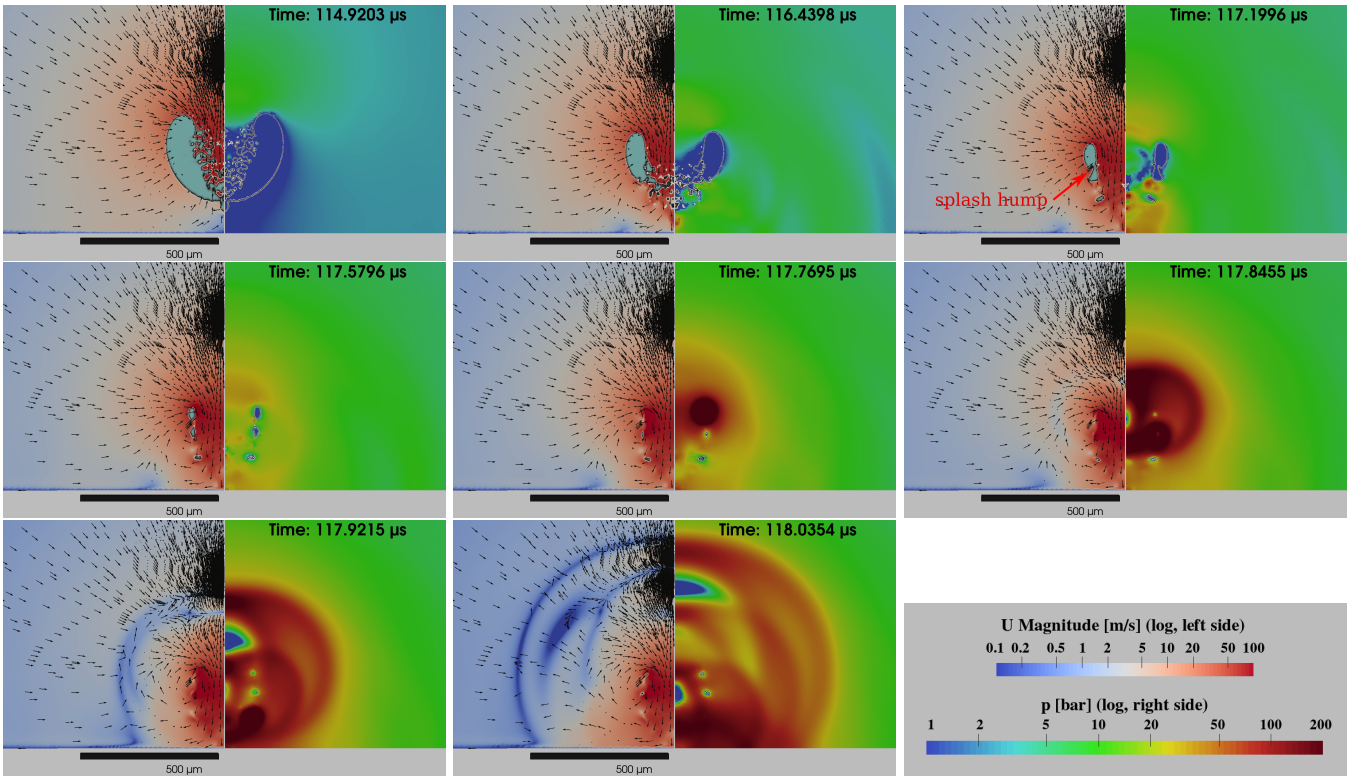

Figure 3: First collapse with torus formation and bubble splitting into three tori, which successively collapse under shock wave emission

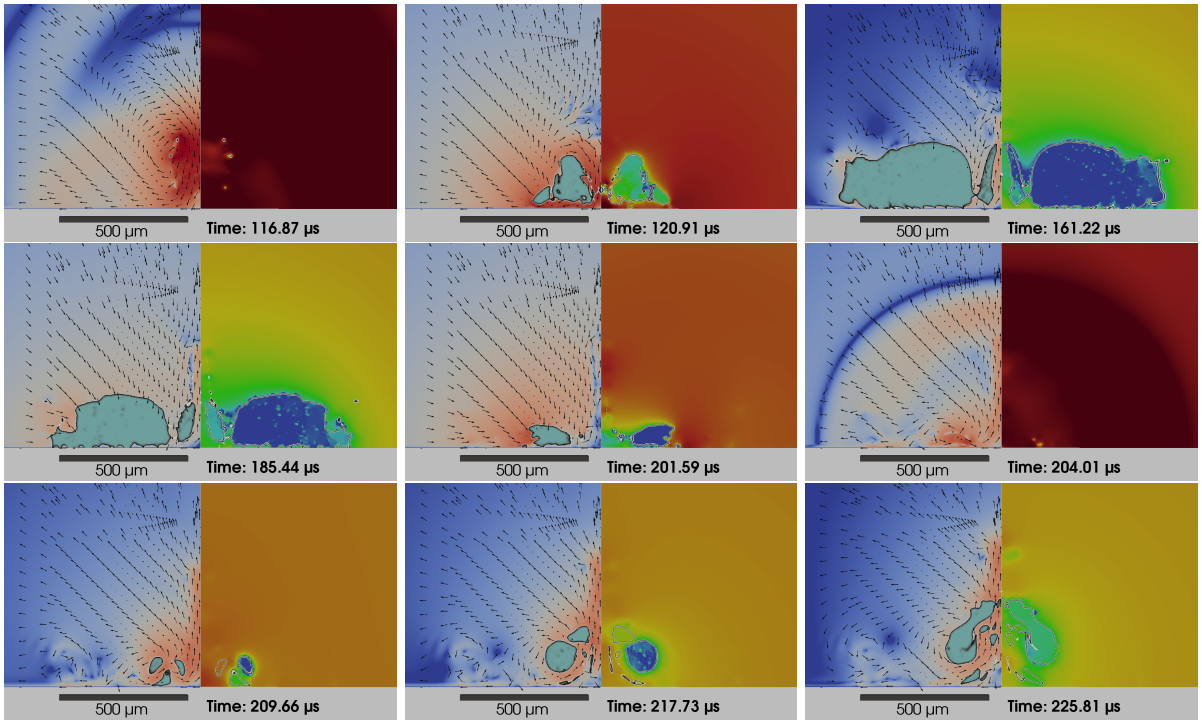

Figure 4: Rebound of the merged tori, second collapse and second rebound; scales are the same as in Fig. 5

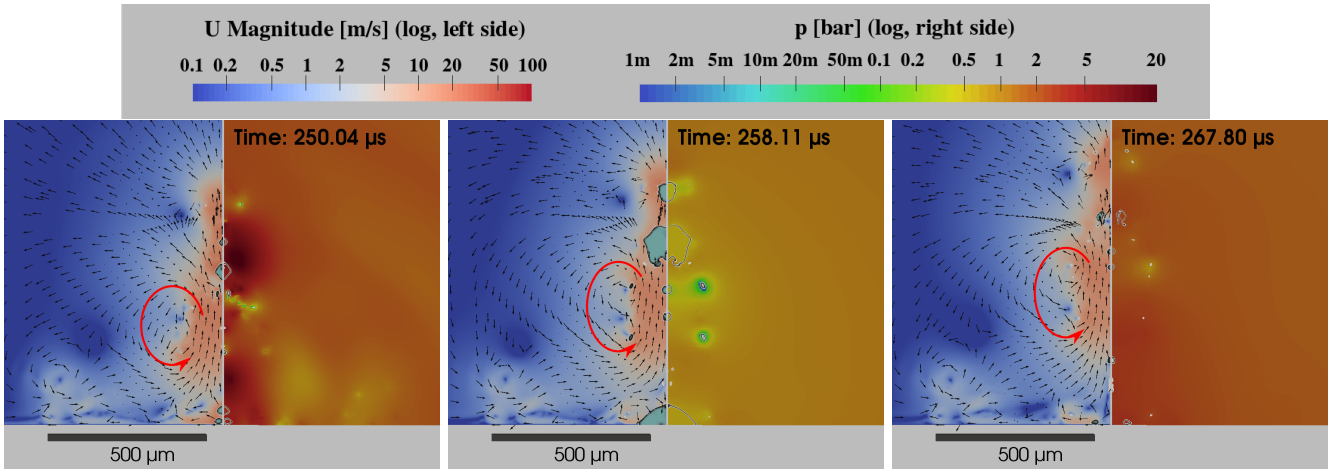

Figure 5: Selected flow vortices

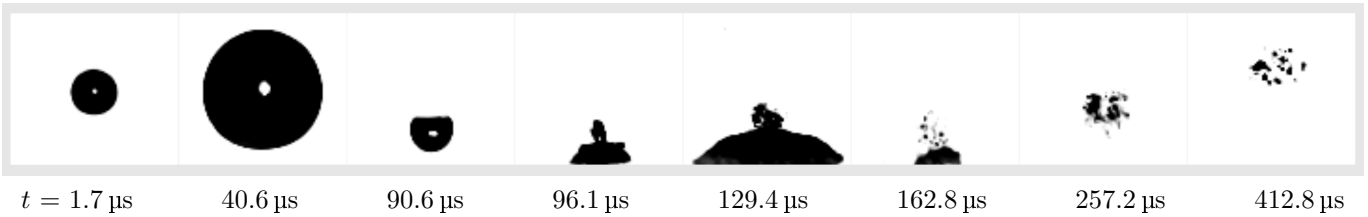

Figure 6: Experimental cavitation bubble with similar standoff-parameter $\gamma_s \simeq 1.20$ compared to calculations ($\gamma_s \simeq 1.17$), solid boundary horizontally at the bottom; $R_{max} = 450\,\mu m$ (≈second frame; simulations: $R_{max} = 550\,\mu m$); collapse time: 93.3 µs (simulations: 117.5796 µs); exposure time $\simeq 370\,ns$